EFFECT OF GRAFTING SOLVENT ON THE OPTIMISATION OF SBA-15 ACIDITY FOR LEVULINIC ACID PRODUCTION

Cristina Pizzolitto[1], Federica Menegazzo[1], Michela Signoretto[1], Alessia Giordana[2], Giuseppina Cerrato[2], Giuseppe Cruciani[3], Elena Ghedini[1]

1 CATMAT Lab, Department of Molecular Sciences and Nanosystems, Ca' Foscari University of Venice and INSTM RUVe, via Torino 155, 30172 Venezia Mestre, Italy

2 Chemistry Department, University of Turin and NIS Interdept. Centre and INSTM RUTo, Via P. Giuria 7, 10125 Torino, Italy

3 Physics and Earth Sciences Department, University of Ferrara, Via Saragat, 1-44122 Ferrara, Italy

Valorisation of lignocellulosic biomass for the production of chemicals is one of the main challenges of the 21st century. Levulinic acid (LA) has been chosen as target product due to its potential as intermediate to produce a crowd of other chemicals. The attention has been focused on the formulation of an acid active catalyst for the hydrolysis of glucose to LA. Therefore, a dee modification of SBA-15 with sulfonic groups using post-synthesis grafting method was performed. In particular, this work focuses on the role of different grafting solvents. The traditional solvents are toluene or hexane, which are flammable and toxic. For this reason, investigation on a safer and more environmentally friendly solvent, a mixture of water and NaCl, has been carried out. It was found that the nature of the solvent highly affects morphological and chemical features of the materials; the best catalytic results were obtained with the catalyst prepared in water and NaCl, as this mixture allows to guarantee the best distribution of sulfonic groups over the surface, leading to the most balanced acid catalyst.

The transformation from a fossil fuel based economy to one based on renewable resources is one of the greatest challenges of the 21st century. Biomass utilization has gained considerable interest in this sense, for its high potentiality as a resourceful substrate for chemical production. Levulinic acid (LA) is considered by the USA Department of Energy, one of the top twelve bio-based building blocks[1] since it can be converted in a great number of bio-chemicals such as succinic acid, resins, polymers, pharmaceuticals, food flavouring agents, herbicides, plasticizers, solvents, and anti-freeze agents[2]. Historically, LA was produced by fossil sources via maleic anhydride[3]; nevertheless, from the second half of the 20th century, the production of levulinic acid has been dominated by biomasses, that is by conversion of carbohydrates or hexose sugars[4]. Indeed, glucose, the most common monosaccharide existing in nature, can be converted into LA through a complex mechanism, including isomerization to fructose followed by dehydration of the ketose monomer to 5-(Hydroxymethyl)furfural (5-HMF) and the subsequent rehydration of the furfural compound to form LA and an equivalent of formic acid (FA)[5]. The catalyst has a pivotal role in this reaction pathway since Lewis acids catalyze the first isomerization step, dehydration of fructose is catalyzed by both Lewis and Brønsted acid sites, while the last step of rehydration of 5-HMF is catalyzed by Brønsted sites[6,7]. Nevertheless, homogenous mineral acids still remain the industrial catalysts used in the transformation of biomass derivatives into LA[8,9,10]. Despite their cheap nature and their catalytic efficiency, researchers are focusing on the development of more sustainable and recyclable heterogeneous systems[11]. Several solid acid materials have been investigated for LA production starting from ion-exchange resins, zeolite, sulfated zirconia, ion-exchange heteropolyacids, and sulfonated solids[12,13,14,15]. Among these, ordered mesoporous silica (OMS) materials, which have already been used in the production of other biofuels, have caught our

attention since they have a high surface area, large pore size distribution and can be easily modified in view of the abundant silanol groups over the surface[16]. SBA-15, among the several OMS, has the suitable properties for biomass exploitation since it has large pore size and thick pore walls[17]. Moreover, it is possible to increase SBA-15 acidity by introduction of acid properties via functionalization with sulfonic acid groups. Different methods can be used to introduce sulfonic sites; the various approaches can involve either direct synthesis, mainly consisting of co-condensations methods, or post-synthesis techniques, as the grafting method or the incipient wetness impregnation. The direct synthesis method in many cases leads to loss of the mesoscopic order of the pore architecture, due to the strong synthetic conditions[18,19]. Considering the post-synthesis approach, the introduction of sulfonic groups is usually performed in concentrated sulfonic acid by heating, which is dangerous and unsustainable[20]. An effective alternative to the direct sulfonation method is the surface alkoxysilanes grafting. It consists of a post-synthesis strategy, by which the active functionalities are anchored on the support surface via covalent bonds. This process is generally carried out in the presence of a grafting agent, such as 3-mercaptopropyltrimethoxysilane (MPTMS), the silica matrix and the solvent[21]. The traditional one is toluene, which is flammable, toxic and not environmentally friendly[22]. For this reason, the investigation of a safer solvent could be an attractive alternative to make this process more sustainable. Indeed, different solvents were evaluated: toluene, as standard reference, hexane to compare the traditional one with another apolar solvent and, a mixture of water and NaCl since it is cheap, natural, not toxic and safe. This research focuses on the investigation of the role of the solvent on the effectiveness of the grafting procedure. In particular, modification of the SBA-15 material has been performed in order to increase its acidity and use this catalyst for LA production.

Experimental part:

Catalyst preparation:

SBA-15 synthesis

Mesoporous SBA-15 was synthesized according to Zhao *et al.*[23] using TEOS (Tetraethyl orthosilicate) as silica source, P123 (EO_{20}-PO_{70}-EO_{20}) as template in acid solution. The mixture was continuously stirred for 24 h at 25 °C and crystallized in a Teflon autoclave at 90 °C for 42 h. The mixture was then filtered, washed, dried at 80 °C for 20 h and finally calcined in air (50 mL/min) at 500 °C for 6 h.

Grafting sulfonic groups

A post-grafting method was used to functionalize the above SBA-15 material. (3-Mercaptopropyl)trimethoxysilane (MPTMS, 95 % Merck) was used as grafting agent meanwhile three different solutions were used as reaction solvent:

1) Toluene: 1 g of SBA-15 was dissolved in 30 mL of toluene. MPTMS was added in a SiO_2/MPTMS = 2 molar ratio. The obtained suspension was refluxed at 120 °C for 24 h.
   After filtration of the resulting thiol-functionalized solid, it was washed with methanol and dried for 18 h at 70 °C. After this step, thiol groups were converted to -SO_3H moieties by mild oxidation with 30 wt% H_2O_2 (molar ratio SiO_2:H_2O_2 = 2:0,11), stirring for 24 h at 30 °C. The sulfonated solid was filtered, washed with methanol and dried at 25 °C for 18 h.
   The final catalyst was labeled SBA-TO.
2) Hexane: 1 g of SBA-15 was dissolved in 30 mL of hexane. As before, MPTMS was added in a SiO_2/MPTMS = 2 molar ratio. The suspension was refluxed at 70 °C for 24 h.
   After filtration of the resulting thiol-functionalized solid, it was washed with methanol and dried for 18 h at 70 °C. Then, mild oxidation with 30 wt% H_2O_2 (molar ratio SiO_2:H_2O_2 = 2:0,11) was performed stirring for 24 h at 30 °C. The sulfonated solid was filtered, washed with methanol and dried at 25 °C for 18 h.
   The final catalyst was labeled SBA-HEX.

3) Saline solution: 1 g of SBA-15 was dissolved in 30 mL of saline solution 0.2 M. MPTMS was added in the proper molar ratio ($2SiO_2$: 1MPTMS) and stirred for 24 h at 90 °C. The solid was then washed in water and dried for 18 h at 70 °C. Then, mild oxidation with 30 wt% H_2O_2 (molar ratio SiO_2:H_2O_2 = 2:0,11) was performed stirring for 24 h at 30 °C. The sulfonated solid was filtered, washed with methanol and dried at 25 °C for 18 h.
The final catalyst was labeled SBA-NaCl.

Characterization

X-ray powder diffraction (XRD) analyses were carried out by a Bruker D8 Advance diffractometer equipped - with a Si(Li) solid state detector (SOL-X) and a sealed tube providing Cu Kα radiation at an accelerated voltage of 40 kV and an applied current of 30 mA.

TEM images were obtained by means of a JEOL 3010–UHR Instrument equipped with a LaB_6 filament (acceleration potential 300 kV) and fitted with an Oxford INCA Energy TEM 200 energy dispersive X–ray (EDX) detector. Samples were dry dispersed onto Cu grids coated with "lacey" carbon film before the analysis.

Specific surface areas and pore size distributions were evaluated from N_2 adsorption/desorption isotherms at -196 °C using a Tristal II Plus Micromeritics. Surface area was calculated using the B.E.T. method[24] whereas pore size distribution was determined by the B.J.H. method[25], applied to the N_2 desorption branch of the isotherm.

Fourier transform infrared (FTIR) spectra were obtained with a Bruker Vector 22 spectrometer equipped with a MCT detector, at 2 cm^{-1} resolution and accumulating 128 scans. The solid samples, in form of self-supported pellets (~10 mg cm^{-2}), were inserted in a conventional quartz vacuum cell equipped with KBr windows connected to a glass vacuum line (residual pressure < 10^{-5} Torr) that allows to perform in situ adsorption/desorption runs. Prior to adsorption/desorption experiments of 2,6-dimethylpyridine (2,6-DMP), all samples were activated at 300 °C in an oxidizing atmosphere. 2,6-DMP adsorption/desorption tests were carried out at 25 °C. First a relatively large amount of base (~ 4 Torr) was allowed on the samples and left in contact for 2 min in order to reach a complete 2,6-DMP monolayer formation, and then the 2,6-DMP excess was evacuated for increasing times in the 1-15 min range in order to put into evidence only the more strongly held fraction.

Thermal analyses (TG/DTA) were performed on a NETZSCH STA 409 PC/PG instrument in air flux (20 mL/min) using a temperature rate set at 5 °C/min in the 25–800 °C temperature range.

Raman spectra were recorded on pure samples using with a FT-Raman Instrument (Bruker Vertex 70 spectrometer, equipped with the RAMII accessory) by exciting with a 1064 nm laser, recording 3000 scans with a resolution of 4 cm^{-1}.

Total Brønsted -acid sites were determined by the following titration method: 50 mg of catalyst was added to a 20 mL sodium hydroxide aqueous solution (0.002 M) and the mixture was stirred for 1 h at RT. After solid filtration, the solution was titrated using a hydrochloric acid aqueous solution (0.002 M). The number of Brønsted acid sites was estimated from the difference between the total amount of base and acid used during the titration, respectively.

Catalytic test

The catalysts were tested for glucose and fructose hydrolysis in a batch stainless still autoclave with mechanical stirring and electric heater. Before the reaction, 500 mg of substrate, 100 mL of water and 200 mg of catalyst were loaded into the reactor and then heated to 180 °C under 10 bar of N_2. The initial time of the reaction is taken once the reaction temperature is reached. The reaction was carried out for 5 hours at

1000 rpm. After this time, the mixture was cooled down to 25 °C and separated by filtration. Reaction mixture was analyzed by high performance liquid chromatography (HPLC) Agilent Technology 1260 Infinity II, equipped by an Aminex HPX-87H column kept at 50 °C. The mobile phase was 5 mM H_2SO_4 with a flow rate of 0,6 mL/min. UV-Vis detector (ʎ = 195 nm) was used for analytes' identification and quantification.

Reactivity parameters were calculated as follows:

$$Conversion\ (\%) = \frac{(mmol\ sub\ in) - (mmol\ sub\ out)}{mmol\ sub\ in} \cdot 100$$

$$Yield\ (\%) = \frac{mmol\ i\ out}{mmol\ sub\ in} \cdot 100$$

Where *i* represents a general product of reaction.

Results and discussion

Preliminary characterisations

Figure 1 shows the low angle XRD patterns of pristine SBA-15 and the corresponding sulfonated materials. SBA-15 evidences three refraction peaks: the main one at 0.95 ° and two smaller at 1.64 ° and 1.85 °, associated with (100), (110) and (200) planes, respectively. This diffraction profile is associated with the 2D-hexagonal *p6mm* pore structure of SBA-15 materials. The presence of the same reflections in the promoted materials confirms that the hexagonal structure is maintained after the incorporation of sulfonic groups as well. Nevertheless, the reflections intensity decreases in the modified samples, especially for SBA-HEX, suggesting that the ordered pore structure could have been affected[26].

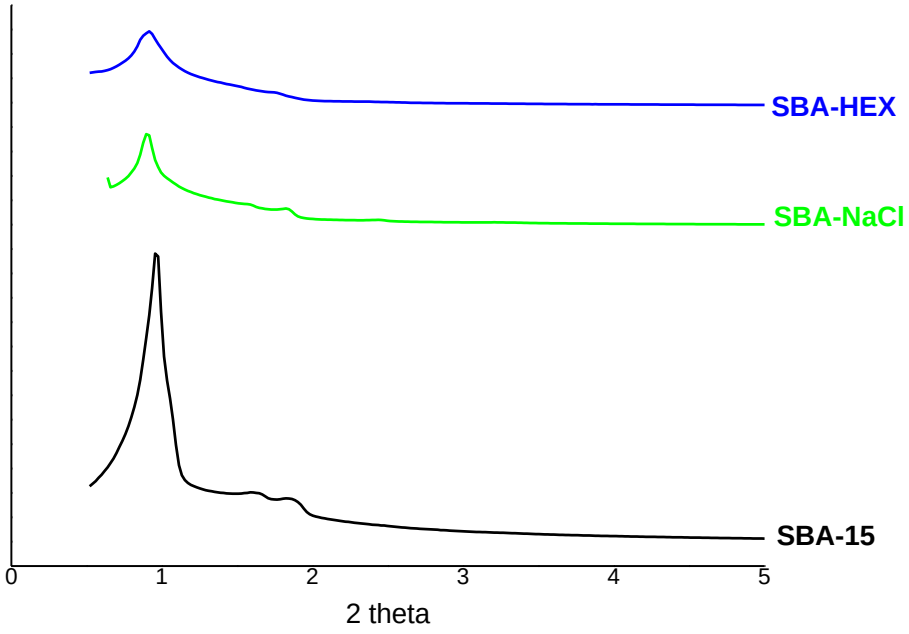

Figure 1 Low-angle XRD patters of pure SBA-15 and grafted SBA-15

The overall morphology of the materials was evaluated by means of both conventional C-TEM and HR-TEM investigations: some selected images have been reported in Figure 2. Plain SBA-15 sample (see Figure 2 section a))exhibits the typical 2D periodic hexagonal structure expected or this material. In the case of all the grafted materials, the highly-organized mesoporous channels are almost totally preserved but, as already highlighted by XRD spectra, the morphology of sulfonated samples is somewhat altered in comparison with pure SBA-15 and a decrease in space order is visible: seesections b, c andd in Figure 2).

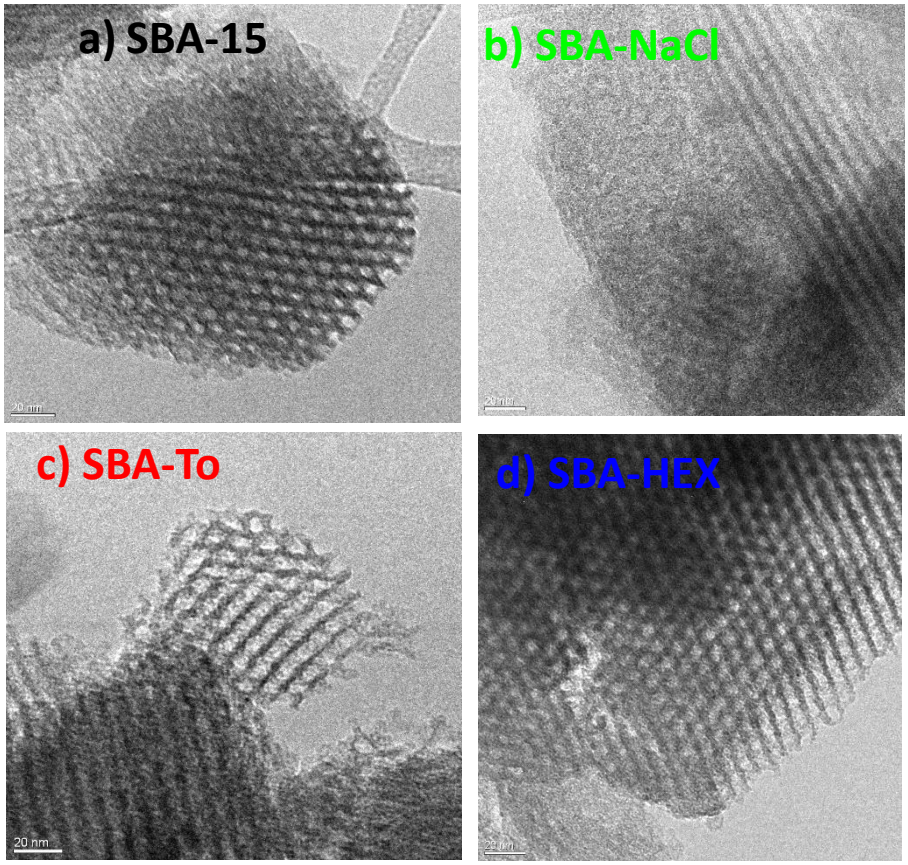

Figure 2 TEM images of a) SBA-15, b) SBA-NaCl, c) SBA-TO and d) SBA-HEX

These results suggest that the grafting approach partially affects the mesoporous ordered organization, even though a good order degree is still preserved. Important parameters that should also be evaluated for catalytic application of these materials are surface area and pore size distribution, therefore, the nitrogen adsorption-desorption measurements were carried out. Isotherms and the corresponding BJH pore size distributions for all the examined samples are reported in Figure 3, section a) and section b), respectively. All samples exhibit IV type adsorption isotherm curves with the characteristic hysteresis loop of a mesoporous material; in the case of SBA-15, the loop has a H1 shape, typical of ordered material with a bottle-necked pore opening. For SBA-TO, slight modification of the hysteresis shape is visible meanwhile a complete change in the hysteresis shape for both SBA-NaCl and SBA-HEX is evident. In the last two cases, a H4 loop shape is present. In all the isotherms the condensation step is located in the range of 0.4-0.8 P/P_0 values. SBA-NaCl and SBA-HEX present a slight shift to lower relative pressures, indicating a lights decrease in the pore diameter. Specific surface area calculated with the BET method and mean pore diameter obtained by BJH method are reported in Table 1. A decrease in BET surface area values, associated with a slight narrowing of the pore diameters, is observed moving from pure SBA-15 to the grafted samples, with the following order: SBA-TO> SBA-NaCl and SBA-HEX, respectively. As reported by other authors[19], the decrease in surface area and pore diameter values can relate with the effectiveness of the grafting approach and in particular to the sulfonic group amount, since grafting reactions could not only proceed at the surface of the material but also inside the pore cavities. Moreover, the change in the hysteresis shape for both SBA-NaCl and SBA-HEX can be a further confirmation of the introduction of alkyl chain of MPTMS precursor inside the pore structure[27].

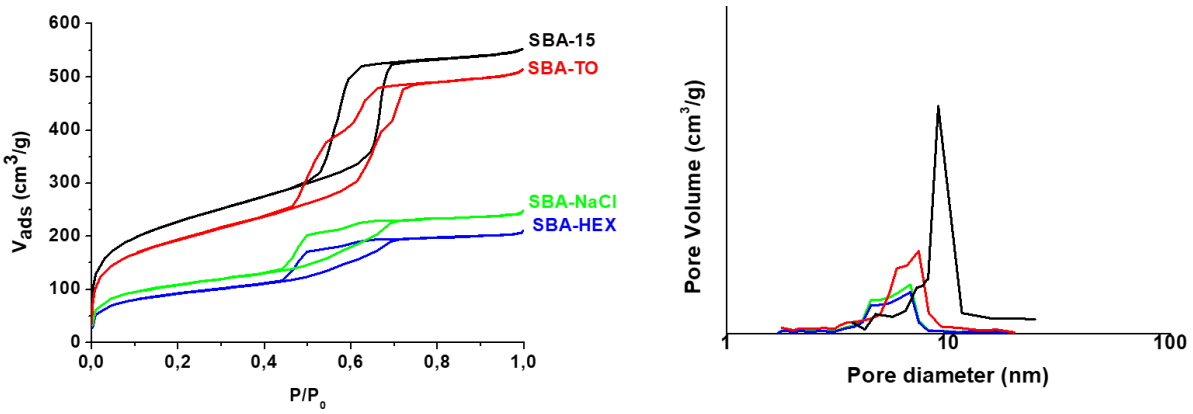

Figure 3 N_2 adsorption-desorption isotherms (left) and pore size distribution (right) of pristine and grafted SBA-15

Table 1 Physical properties of pristine and grafted SBA-15.

Samples	A_{sup} (m^2/g)[a]	Pore diameter (nm)[b]	Weight loss (%)[c]
SBA-15	866	5.3	-
SBA-To	655	5.4	13 %
SBA-NaCl	393	4.7	17 %
SBA-HEX	288	4.7	14 %

[A] Specific surface area (m^2/g) calculated via BET equation

[B] Pore diameter (nm) calculated via BJH equation

[C] weight loss (%) determined by thermogravimetric analysis

FTIR analysis was carried out as qualitative method for the identification of the surface functionalities of the material. Figure 4 reports FT-IR spectra of both pristine support and grafted materials after the thermal activation:no undissociated adsorbed water is present yet, even though in the 3900-2800 cm^{-1} spectral range (ν_{OH}) it is possible to recognize two peculiar contributions. The band at higher frequency (~3740 cm^{-1}) can be ascribed to the ν_{OH} mode of terminal silanols free from H-bonding interaction, and a broad and unresolved envelope located at lower wavenumber due to the ν_{OH} of hydroxyl groups still interacting by H-bonding.[33] While the signal due to terminal silanols is well resolved in SBA-15 spectrum and the unresolved envelope represents a minor spectral feature, for all the grafting materials this broad envelope is well evident even after thermal activation and represents the predominant spectral component, suggesting a major hydrated surface where many OH groups may still interact by H-bonding. Nevertheless, for SBA-NaCl the peak of terminal silanols is less intense in comparison with the other sulfonated materials, suggesting that a major interaction of silanos groups with MPTMS has occurred during the synthesis. Moreover, the presence of sulfonated species is confirmed by the spectral component located at ~ 1375 cm^{-1} (see the inset to Figure 4), which can be ascribed to asymmetric stretching of these moieties. The intensity of this peak is slightly higher for the SBA-NaCl sample than the corresponding one of SBA-TO and SBA-HEX, indicating the possible presence of a larger amount of sulfonated groups for the SBA-NaCl material.

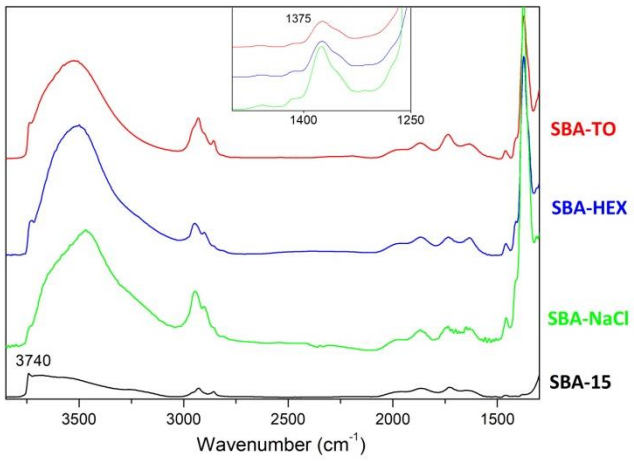

Figure 4 FT-IR spectra of samples after thermal treatment in vacuum

To clearly quantify the number of these sulfonated groups on the silica surface, TG-DTA analysis was performed. In Figure 5 the percentage weight loss and the exchange heat in the left and right ordinate respectively, as a function of the temperature, have been reported. For all the samples, a weight loss associated with an endothermic heat transfer is visible below 150 °C; this can be attributed to the removal of adsorbed water.

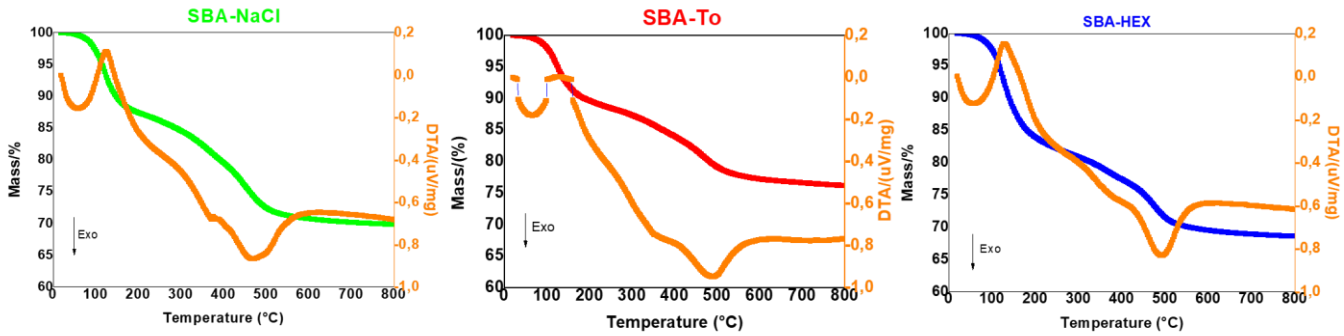

Figure 5 TG-DTA analysis of SBA-NaCl, SBA-TO and SBA-HEX catalysts.

For all the samples, it is also visible a second exothermic component in the 350 – 600 °C temperature range. This peak is associated with the decomposition of alkyl sulfonic acid group in C_3H_6, SO_2 and H_2O; therefore, as reported by P. Zhang *et al.*[19], the amount of weight loss in this temperature range can be correlated with the number of sulfonic groups grafted on the material surface. As reported in Table 1, the catalyst prepared in saline solution (SBA-NaCl) presents the most remarkable weight loss, so the highest amount of the sulfonated species anchored on the support. Hexane solvent makes the grafting less effective, meanwhile the most traditional solvent, toluene, seems to be the least efficient. Thermal analysis results also confirm the effectiveness of the oxidation step, since no peaks associated with the oxidation of thiol species to sulfonic groups are present. In this regard, Figure 6 reports the TG-DTA analyses conducted on the materials before the H_2O_2 treatment. Mercaptopropyl groups decompose at 350 °C and in Figure 6 a broad exothermic peak between 200-600 °C is visible, associated firstly with the thiol (-SH) and disulphide (-S-S-) decomposition, followed by the decomposition of propyl sulfonic acid group above 350 °C[22]. The difference between the not oxidized (Figure 6) and oxidized samples (Figure 5) is evident since, in the last case, the range of temperature associated with the endothermic peak is sharper and located at higher temperature.

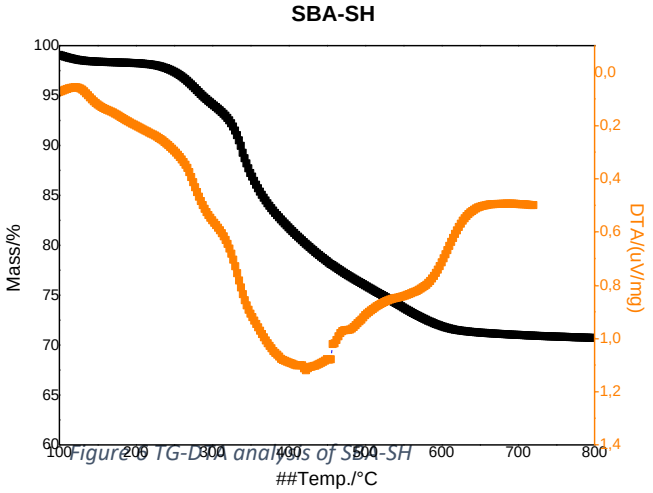

Figure 6 TG-DTA analysis of SBA-SH

Further investigation was performed via Raman spectroscopy to definitively exclude the presence of unreacted –SH groups, as Raman spectroscopy is very sensitive toward thiol vibrations. In Figure 7, the comparison among the Raman spectra of SBA-15, SBA-SH and the sulfonated materials is reported in Figure 7.

The SBA-15 spectrum exhibits five weak signals at low wavenumbers. It is very similar to that of pure silica, but for the intensity of the peak at 980 cm^{-1} (see the magnified black curve in Figure 7), ascribable to surface silanol groups, that becomes more relevant in mesoporous systems[28].

On the contrary, the spectrum of grafted-MPTMS (SBA-SH) sample exhibits a strong band at ~ 2570 cm^{-1}, ascribable to the ν_{S-H} stretching mode of the mercaptopropyl segment present in MPTMS; moreover, it is possible to observe a band at 651 cm^{-1}, that is assigned to the ν_{C-S} stretching mode[29]. The formation of bridged disulfide groups can be excluded due to the absence of modes in the 500-550 cm^{-1} spectral range[30]. Thus, it can be concluded that the thiol group is grafted to the SBA-15 material without any chemical alterations.

Raman spectra relative to samples after oxidation with H_2O_2 are very similar each other and confirmed the complete transformation of the thiol functionality into -SO_3H groups according with thermal analyses: see the green, blue and red curves in Figure 7 .

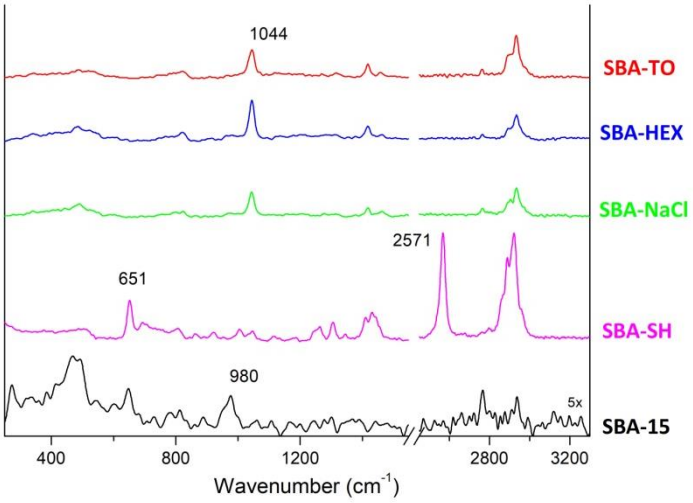

Figure 7 FT-Raman spectra

It is possible to observe the disappearing of the thiol stretching mode at ~ 2570 cm^{-1} with th parallel appearance of a new signal at 1044 cm^{-1}, ascribable to the symmetric mode of the SO_3 group of the

corresponding sulfonic acid[31]. On the contrary, the formation of disulphide species can be excluded also in oxidized samples. In conclusion, the Raman technique allows to exclude the presence of unreacted thiols group and to verifythe efficiency of H_2O_2 oxidation treatment.

Reactivity

After preliminary characterisations, catalytic tests were carried out. All these materials were tested in the hydrolysis reaction with two different substrates, glucose and fructose. Figure 8 reports fructose conversion and products yield in section a) while glucose conversion and its products yield are reported in section b).

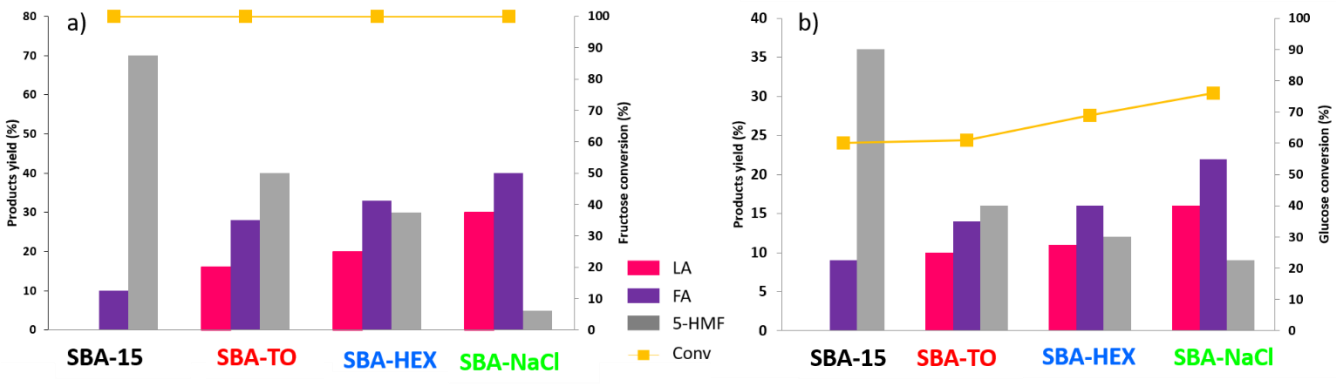

Figure 8 Substrate conversion (Section a): Fructose, Section b): Glucose) and products yield as a function of different catalysts. Reaction conditions: 180 °C, 10 Bar of N_2 for 7 h.

As reported by Ramli *et al.*[32], glucose isomerization to fructose is the rate determining step of the glucose hydrolysis reaction. Therefore, as evident in section a) of Figure 8, 100% of conversion has been obtained for all the catalysts using fructose as substrate. The main differences between them can be found in the products yield. For pristine SBA-15, no levulinic acid production is ever obtained. SBA-15, as previously reported, owns an intrinsic Lewis acidity given by the silanols functionalities, whereas the absence of Brønsted acid sites does not allow the hydration of 5-HMF, the main product, to LA. On the contrary, the reaction is complete in the case of sulfonated materials. In particular, for both SBA-TO and SBA-HEX a very similar behaviour can be observed, whereas SBA-NaCl reaches 30 % of LA yield, 40 % of FA yield and only 6 % of 5-HMF yield. in this last case, hydration of 5-HMF to LA is favoured in comparison with the catalysts prepared in apolar solvents,. Similar trend has been found for glucose hydrolysis, as reported in section b) of Figure 8. Firstly, it must be pointed out that, no complete conversion is ever achieved using glucose as substrate. The maximum value (80 %) is obtained with SBA-NaCl . Even in this case, SBA-NaCl exhibits the highest LA yield and the lowest amount of 5-HMF.

In order to understand the role of the solvent in the catalytic results, the acidity of the samples was evaluated by both titration and FTIR with a basic probe molecule.

Acidic properties

Table 2 summarizes the evaluation of the acidic properties of the SBA-based materials.

Table 2 Acidic properties of pristine and grafted SBA-15

	Acid capacity (mmol/g)[b]	L/B[a]
SBA-15	-	∞

SBA-NaCl	10	1,6
SBA-HEX	6.4	1,9
SBA-TO	7.8	1,8

[a] Ratio between Lewis and Bronsted acid sites calculated on normalized spectra using ε_L=1,9 and ε_B=7,9, as determinate by ref.[34]
[b] Acid capacity (mmol/g) calculated via titration method

For the total acidity, evaluated by titration method, the material prepared in saline solution (SBA-NaCl) presents the highest value followed by the catalyst prepared by using the most traditional solvent, toluene. It is important to underline that, this test gives only a roughly determination of acidity without properly distinguishing between Lewis and Brønsted acid sites. In order to evidence both kinds of acidity of the catalysts, FTIR adsorption of 2,6-dimethylpyridine (2,6-DMP) was carried out at ambient temperature. FTIR spectra of 2,6-DMP adsorbed on all samples are presented in figure 9, in the spectral range of signals ascribable to 8a and 8b modes of 2,6-DMP following a well accepted procedure reported in the literature [33].

.

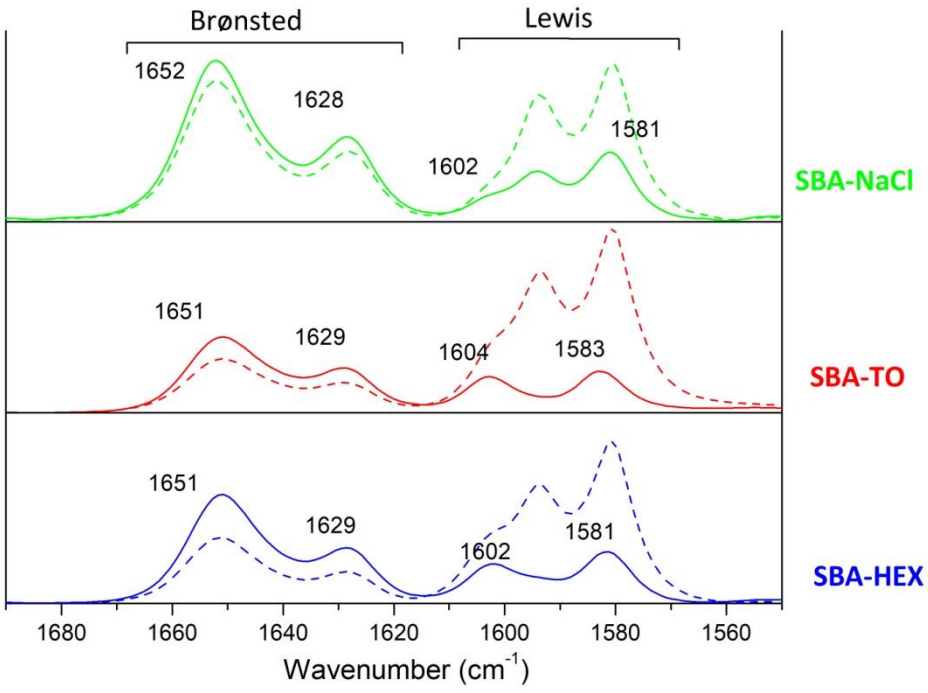

Figure 9 FT-IR spectra of adsorption/desorption of 2,6-DMP (dash line under maximum pressure of 2,6-DMP, line after evaluation for 15 min) for SBA-HEX, SBA-TO and SBA-NaCl.

In all samples, 2,6-DMP adsorption/desorption spectra suggest the presence of Brønsted acidic centers, whose signals at ~1650 and 1630 cm^{-1} increase in intensity after evacuation for 15 minutes. At lower wavenumbers, 8a and 8b modes of physisorbed and H-bonding 2,6-DMP (1604, 1595 and 1580 cm^{-1}) are detectable: only signals still present after evacuation are attributable to Lewis acid sites of medium-high strenght, as these are more strongly held at the surface. On the contrary, 2,6-DMP adsorption on SBA-15 (not shown for the sake of brevity) reveals the presence of only Lewis acidic sites, but no signals attributable to Brønsted centers are detectable, in good agreement to literature data on silica-based materials[33]. As already reported in the "Reactivity" section for what concerns glucose/fruttose hydrolysis, selectivity is influenced by both strength and number of Lewis and Brønsted acid sites, thus the ratio between Lewis and Brønsted acidic sites (L/B) could play a key role in determining the best catalyst The estimation of (L/B) ratio requires the knowledge of molar absorption coefficients (ε) values, specific for

each vibrational mode considered and influenced by the surface. Some studies suggest that a little variation of ε as a function of the type of solids and estimated ε values for 2,6-DMP adsorbed through H-bonding, coordination and protonation [34,35]. To minimize errors deriving from average values (reported approximately to be 18%)[34,35], in the present aproach the molar absorption coefficient determinated for the 8a and 8b modes on similar materials (silica and phosphate silica) have been taken into account[34.] Calculated L/B ratios for the SBA-based samples (reported in Table 2) are higher than unity for all samples suggesting a prevalence of Lewis acidity, but differences among samples are quite evident. Samples treated with apolar solvents, present similar values while in the case of saline solution the lower value of this ratio suggests a higher amount of Brønsted acid sites. These results agree with the acid capacity obtained via titration method: the L/B ratio decreases as the acid capacity increases.

Preliminary characterisations and acid properties analyses allow to discriminate the effect of solvents: the use of saline solution, in comparison with apolar traditional solvents, increase the number of sulfonated molecules over the surface bringing to higher Brønsted acidity. As reported by Pirez *et al.*[36], since SBA-15 is already calcined before the grafting treatment, it exhibits an insufficient number of free surface silanols. The solvent effect can be founded in the ability of NaCl to open Si-O-Si bonds, restoring a suitable number of free Si-OH in the presence of Cl^- before the nucleophilic substitution with MPTMS. Indeed, the modification of SBA-15 materials in saline solution increases the accessibility of silanols, leading to a higher sulfonation. The catalytic results are in good agreement with what is obtained from acidity characterizations as a direct correlation between catalyst acidity (L/B) and LA yield is evidenced. Indeed, SBA-NaCl, exhibiting the highest total acid capacity, calculated via titration, besides the lowest L/B ratio, can promote the last stage of reaction ,ruled by Brønsted acidity, reaching the highest LA yield.

Conclusions

Herein, sulfonic acid SBA-15 materials were successfully prepared for the conversion of glucose to levulinic acid. Materials were preprared via post-synthesis grafting using three different solvents: toluene, hexane and water/NaCl. The effect of the solvents has been evaluated pointing the attention on morphological and structural features and acidic properties. It was found that the grafting approach only affects, partially, the mesoporous ordered organization, still preserving a good order degree. However, the solvent effect strongly impacts on the success of grafting procedures. Indeed, the use of saline solution, in comparison with apolar traditional solvents, leads to increase the number of sulfonated molecules over the surface bringing to higher Brønsted acidity. This fact has a direct effect on catalytic activity in the glucose and fructose hydrolysis . Best catalytic results were obtained for both reagents using using water/NaCl as grafting solvent. Indeed, this material favours the rehydration reaction of 5-HMF, leading to the highest LA yield. It was therefore possible to increase the efficiency of post-synthesis grafting approach using a sustainable, economic and environmentally friendly solvent.

[1]T. Werpy, G. Petersen, Top Value Added Chemicals from Biomass: Volume I -- Results of Screening for Potential Candidates from Sugars and Synthesis Gas. United States: N. p., 2004. Web. doi:10.2172/15008859.
[2] S.S. Chen, T. Maneerung, D.C.W. Tsang, Y.S. Ok, C. Wang, Chem. Eng. Sci. 328 (2017) 246-273.
[3] A. M. Raspolli Galletti, C. Antonetti, V. De Luise, D. Licursi, N. Nassi, Bioresources 7(2) (2012) 1824-1835.
[4] A. Morone, M. Apte, R.A. Pandey, Renew. Sust. Energ. Rev. 51 (2015) 548-565.
[5] A. Mukherjee, M. Dumont, V. Raghavan, Biomass Bioenergy 72 (2015) 143-183.
[6] R. Weingarten, J. Cho, R. Xing, W. Conner, G. Huber. ChemSusChem 5 (2012) 1280–1290.
[7] K. Kohli, R. Prajapati, B. K. Sharma, Energies 12 (2019) 233-273.

[8] S.W. Fitzpatrick, ACS Symposium Series Feedstocks for the Future (2006) 271–287
[9] S. Kang, J. Fu, G. Zhang, Renew. Sust. Energ. Rev. 94 (2018) 340-362.
[10] H. Jeong, S. Jang, C. Hong, S. Kim, S. Lee, S. Min Lee, J. Weon Choi, I. Choi, Bioresour Technol. 225 (2017) 183-190.
[11] I. Thapa, B. Mullen, A. Saleem, C. Leibig, R. Tom Baker, J. B. Giorgi, Appl. Catal. A. 539 (2017) 70-79.
[12] Y. Zhang, Q. Xiong, E. Zhu, M. Liu, J. Pan, Y. Yan, Energy Technol. 6 (2018) 1941– 1950.
[13] A. Osatiashtiani, A. F. Lee, D. Robert Brown, J. A. Melero, G. Morales, Karen Wilson, Catal. Sci. Technol. 4 (2014) 333-342.
[14] N.A. Syahirah Ramli, N.A. Saidina Amin, Appl. Catal B. 163 (2015) 487-498.
[15] K. Peng, X. Li, X. Liu, Y. Wang, Molecular Catalysis 441 (2017) 72–80.
[16] V. Chaudhary, S. Sharma, J Porous Mater 24 (2017) 741–74.
[17] J. Wang, H. Ge, W. Bao, Materials Letters 145 (2015) 312–315.
[18] D. Margolese, J. A. Melero, S. C. Christiansen, B.F. Chmelka, G.D. Stucky, Chem. Mater. 12 (2000) 2448-2459.
[19] P. Zhang, H. Wu, M. Fan, W. Sun, P. Jiang, Y. Dong, Fuel 235 (2019) 426-432.
[20] F. Su, Yihang Guo, Green Chem. 16 (2014) 2934-2957.
[21] N. V. Krishana, S. Anuradha, R. Ganesh, V. V. Kumar, P. Selvam, ChemCatChem 10 (2018) 5610-5618.
[22] J. Dhainaut, J. Dacquin, A. F. Lee, K. Wilson, Green Chem. 12 (2010) 296–303.
[23] D. Zhao, J. Feng, Q. Huo, N. Melosh, G.H. Frederickson, B.F. Chmelka, G.D. Stucky, Science 279 (1998) 548
[24] S. Brunauer, P.H. Emmett, E. Teller, J. Am. Chem. Soc. 60 (1938) 309−319.
[25] E.P. Barrett, L.S. Joyner, P.P. Halenda, J. Am. Chem. Soc. 73 (1951) 373−380.
[26] E. Casas, B. Paredes, R. Van Grieken, J. M. Escola, Catal. Sci. Technol. 3 (2013) 2565—2570.
[27] Z. Xue, H. Shang, C. Xiong, C. Lu, G. An, Z. Zhang, C. Cui, M. Xu, RSC Adv. 7 (2017) 20300-20308.
[28] A. S. Cattaneo, C. Ferrara, D. C. Villa, S. Angioni, C. Milanese, D. Capsoni, S. Grandi, P. Mustarelli, V. Allodi, G. Mariotto, S. Brutti, E. Quartarone, Microporous Mesoporous Mater. 219 (2016) 219-229.
[29] K. Möller, J. Kobler and T. Bein, J. Mater. Chem. 17 (2007) 624–631.
[30] H. Okabayashi, K. Izawa, T. Yamamoto, H. Masuda, E. Nishio, C. J. O'Connor, Colloid Polym Sci 280 (2002) 135–145.
[31] K. Wilson, A. F. Lee, D. J. Macquarrie, J. H. Clark, Appl. Catal. A 228 (2002) 127–133.
[32] N. A. Syahirah Ramli, N. A. Saidina Amin, Chem. Eng. J. 335 (2018) 221–230.
[33] C. Morterra, G. Cerrato, G. Maligrana, Langmuir 17 (2001) 7053–7060.
[34] T. Onfroy, G. Clet, M. Houalla, Micropor. Mesopor. Mater. 82 (2005) 99–104.
[35] A. J. McCue, G. A. Mutch, A. I. McNab, S. Campbell, J. A. Anderson, Catalysis Today 259 (2015) 19–26
[36] C. Pirez, A.F. Lee, J.C. Manayil, C.M.A. Parlett, K. Wilson, Green Chem. 16 (2014) 4506-4509.